PROOF-MASS INERTIAL VIBRATION CONTROL USING A SHUNTED ELECTROMAGNETIC TRANSDUCER

Andrew J. Fleming, and S. O. Reza Moheimani *

* *University of Newcastle, Australia*

Abstract: Inertial drives and passive tuned-mass dampers utilize a suspended mass to reduce the vibration experienced by a host structure. Active vibration control systems typically include a voice-coil type electromagnetic actuator to develop the required reaction forces. In this paper, the technique of sensor-less active shunt control is applied to inertial vibration absorbtion. An electrical impedance is designed and connected to an electromagnetic coil with a view to minimizing structural vibration. Standard optimal control tools can be applied to design the required shunt impedance. The technique requires no additional feedback sensors. Vibration in an experimental structure is heavily attenuated by the application of an active shunt impedance. *Copyright©2005 IFAC.*

Keywords: Vibration dampers, Electromagnetic transducers, Inertial Platform, Damping, Active Noise Control.

1. INTRODUCTION

Tuned mass dampers, or inertial drives are commonly used for mechanical vibration control (Rao, 1995; Inman, 2000). Tuned mass absorbers utilize an inertial mass and tuned support to introduce additional dynamics and mitigate vibration over a certain frequency range. Active vibration control systems employ inertial drives to regulate the signal from an accelerometer or related performance signal.

This paper considers vibration reduction using an electromagnetically actuated inertial drive. Both the passive and active drive dynamics are considered when constructing a model of the mated mechanical and inertial drive systems. In doing so, the performance of a passive absorber can be augmented with an active feedback system. A method is presented for the modelling, design, and implementation of a shunt controlled electromagnetic inertial drive for vibration suppression. By viewing the coil current and voltage as system inputs and outputs, the task of impedance synthesis can be cast as a standard feedback design problem. Arbitrary objectives such as LQR, LQG, or $\mathcal{H}_2$ goals are easily specified. In this work, displacement is minimized subject to a penalty on the inertial mass travel and applied terminal voltage. Using this technique, the need for external sensors is eliminated, significantly reducing the cost, complexity, and sensitivity to transducer failure that in many applications, may preclude the use of an active control system.

Experiments are performed on a simple single-mode host structure with integrated electromagnetic transducer and suspended absorber mass. The combination of passive and active control results in significant vibration suppression.

This paper is presented in 5 sections. In Section 2, we begin with the modeling of mechanical, electromagnetic, and composite systems. A method is then presented in Section 3 for the design of active impedance and admittance controllers to
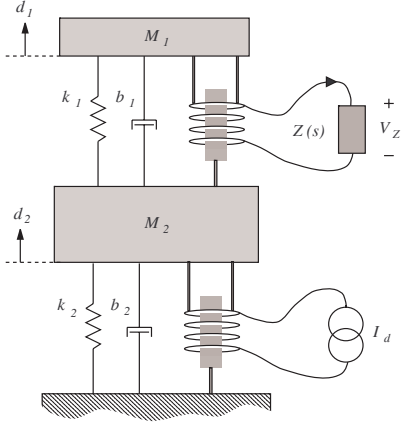
Fig. 1. A two-mass system with electromagnetic transducers to realize the disturbance force F_d and control force F_e.

minimize a specified performance objective. The presented techniques are then applied to an experimental electromagnetic system in Section 4. Finally, the paper is concluded in Section 5.

2. MODELING

As shown in Figure 1, we consider a mechanical system coupled to a shunted electromagnetic transducer. The aim is to reduce vibration in the host system M_2 via the electromagnetically actuated inertial mass M_1. A force disturbance is applied to M_2 via the current I_d. A system block diagram of the mechanical system is shown in Figure 2, a state-space representation is easily obtained.

In Figure 2 the impedance $Z(s)$, interpreted simply as the transfer function relating coil current to terminal voltage, appears analogous to a feedback controller for the electromechanical system. By concatenating the mechanical and electromagnetic systems, P and E, as shown in Figure 3, the composite system is cast as a typical regulation problem for the abstracted system G.

3. CONTROL DESIGN

As shown in Figure 2, an impedance connected to a mechanically coupled electromagnetic transducer can be viewed as parameterizing a velocity feedback controller for the mechanical system P. The following section introduces a technique for the synthesis of active impedance controllers designed to minimize structural vibration.

Our design objective is to minimize the displacement d_2 whilst restraining both the magnitude of control voltage V_z and the absorber mass travel $d_1 - d_2$. As the reaction force F_e results in an
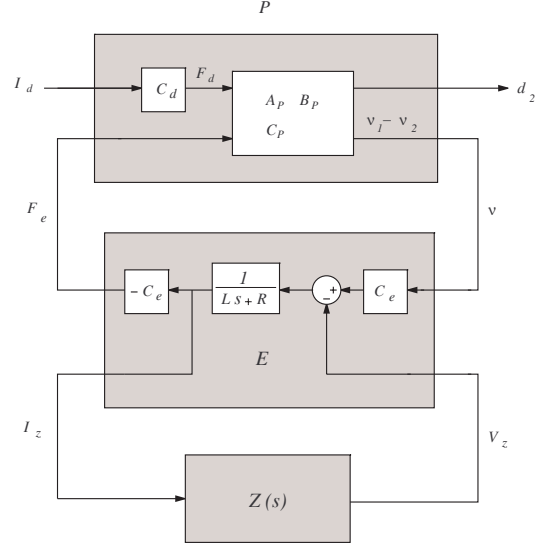

Fig. 2. The mechanical system P coupled to an impedance shunted electromagnetic transducer E. The mechanical system is descibed by A_p, B_p, and C_p. L and R are the inductance and resistance of the coil. C_d and C_e are the electromagnetic coupling coefficients of the force disturbance and control coil.
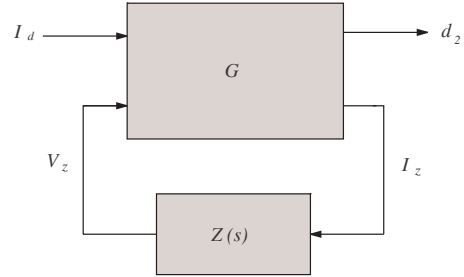

Fig. 3. The composite system G comprising the mechanical and electromagnetic sub-systems.

acceleration of the absorber, at low frequencies the magnitude of available force is strictly limited by the maximum travel $d_1 - d_2$. In a linear quadratic sense, our objective is to minimize

$$J = \int_0^\infty \left\{ d_2^2(t) + k_v V_z^2(t) + k_d \left(d_1(t) - d_2(t) \right)^2 \right\} dt. \tag{1}$$

where k_v and k_d represent weightings on the applied shunt voltage V_z and the absorber mass travel $d_1 - d_2$. By substituting the state solutions into $d_1(t)$ and $d_2(t)$, we obtain

$$J = \int_0^\infty \left\{ x_p'(t) \mathbf{C}_{p1}' \mathbf{C}_{p1} x_p(t) \right. \tag{2}$$
$$+ V_z(t)' k_v V_z(t \tag{3}$$
$$\left. + x_p'(t) \mathbf{C}_{p3}' k_d \mathbf{C}_{p3} x_p(t) \right\} dt. \tag{4}$$

where $d_1(t) - d_2(t) = \mathbf{C}_{p3} x_p(t)$, and $\mathbf{C}_{p3} = \begin{bmatrix} 0 & -1 & 0 & 1 \end{bmatrix}$. Restated in the standard LQR context,
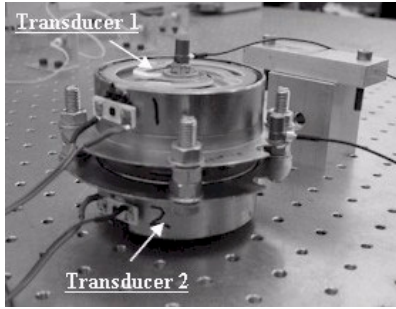
Fig. 4. The experimental apparatus.

$$J = \int_0^\infty \left\{ x_g'(t)\mathbf{Q}x_g(t) + u(t)'\mathbf{R}u(t) \right\} \ dt. \quad (5)$$

where $\mathbf{Q} = \left[\ \mathbf{C}_{p1} \ 0 \ \right]' \left[\ \mathbf{C}_{p1} \ 0 \ \right] + k_d \left[\ \mathbf{C}_{p3} \ 0 \ \right]' \left[\ \mathbf{C}_{p3} \ 0 \ \right]$, and $\mathbf{R} = k_v$.

Through the solution of an algebraic Ricatti equation, a state feedback matrix K can be found that minimizes the objective function J.

3.1 Observer Design

As the state variables of the system $x_g(t)$ are not available directly, a linear observer is required.

For impedance design, the *ad-hoc* pole-placement approach to linear observer design becomes difficult. A more automated choice in observer design is the Kalman filter (Brown and Hwang, 1997). The controller $C(s)$ now consists of an optimal state-feedback regulator K and Kalman observer O. By the Certainty Equivalence Principle or Separation Theorem (Skogestad and Postlethwaite, 1996), the two entities can be designed independently. After first finding a K to minimize (5), we then design a Kalman filter to minimize

$$J_k = \lim_{t\to\infty} E\left\{ [x(t) - \tilde{x}(t)]\,[x(t) - \tilde{x}(t)]' \right\}. \quad (6)$$

4. EXPERIMENTAL RESULTS

To verify the modeling and design techniques presented in the preceding sections, each method has been applied to an experimental electromechanical system. Details of the experimental apparatus, shown in Figures 4 and 5, are discussed in the following subsections.

4.1 Experimental Apparatus

A photograph of the experimental apparatus showing the rigid body, flexible end supports, mounting plate, and coils is provided in Figure 4. As shown in Figure 5, the apparatus comprises two electromagnetic transducers mounted vertically. While the lower magnet and flexure
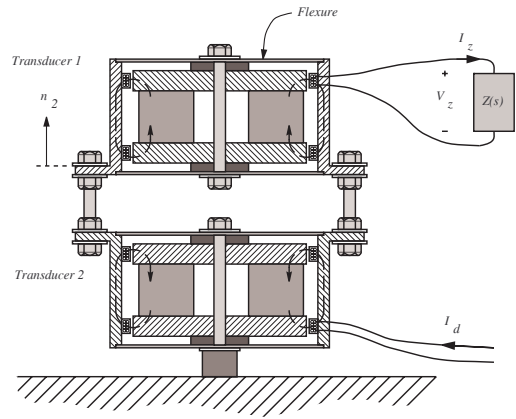

Fig. 5. A crossection of the experimental apparatus shown in Figure 4

Parameter	Value
Spring constant k_1	28.03 kNm^{-1}
Damping coefficient b_1	1.500 Nsm^{-1}
Absorber mass M_1	0.340 kg
Spring constant k_2	31.14 kNm^{-1}
Damping coefficient b_2	3.582 Nsm^{-1}
Absorber mass M_2	0.593 kg
Coil inductance	41 mH
Coil resistance	2.315 Ω
Electromagnetic Coupling C_e	3.408
Electromagnetic Coupling C_d	-6.714

Table 1. Electromechanical system parameters.

is fixed, the two connected transducer cases are free to vibrate and represent the mass M_2. The upper magnet forms the absorber mass M_1. Each transducer is essentially a translational solenoid with two identical coils connected in series, the dashed line identifies the flux path generated by the permanent magnets. The physical parameters of the electromagnetic and mechanical systems are summarized in Table 1.

The main mass velocity d_2 is measured using a PSV-300 Polytec Scanning Laser Vibrometer.

4.2 Power amplifier and instrumentation

In order to implement an arbitrary shunt impedance, a power amplifier was developed capable of driving differential terminal voltages with load current instrumentation. The simplified schematic of a circuit realizing this function is shown in Figure 6.

A practical implementation of the amplifier is shown in Figure 7. The device is capable of $\pm$ 200 V operation at a maximum DC current of 32 Amps. A dSpace 1005 based system is used
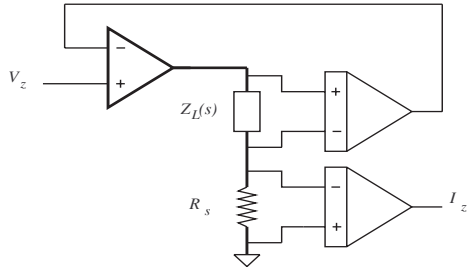
Fig. 6. The simplified schematic of a voltage source with current instrumentation. The load impedance $Z_L(s)$ represents the electromagnetic coil.
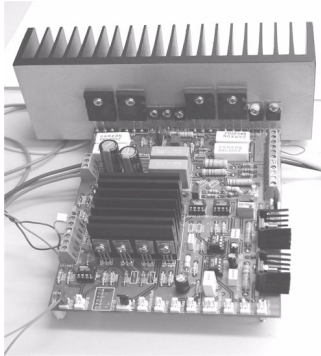

Fig. 7. Practical implementation of a voltage amplifier with current instrumentation.
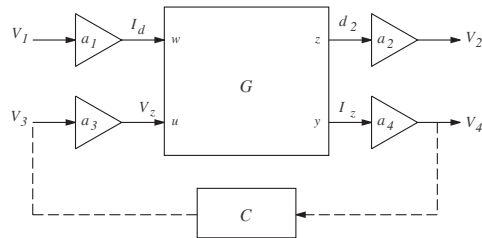

Fig. 8. External gains associated with the amplifier and instrumentation.

to implement the required impedance transfer functions.

4.3 Impedance synthesis

Figure 8 shows the instrumentation and driver gains associated with the underlying electromechanical system. The voltages V_1 through V_4 represent the signals applied to, or measured from, the power amplifiers and instrumentation. The gain and units associated with each signal can be found in Table 2. The actual electrical shunt impedance presented to the coil is related to the controller through the gains a_3 and a_4, specifically,

$$Z(s) = \frac{V_z(s)}{I_z(s)} = a_3 C(s) a_4 \qquad (7)$$

Gain	Value
a_1	1.006 A/V
a_2	1 V/m
a_3	-1.012 V/V
a_4	-10.01 V/A

Table 2. External gains associated with the experimental system
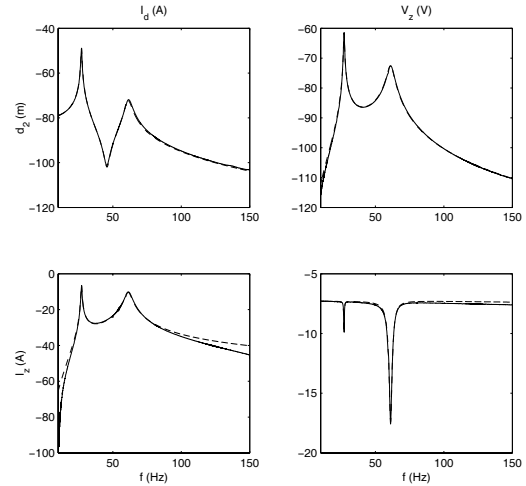

Fig. 9. The simulated (—), and experimental (- -), magnitude frequency response.
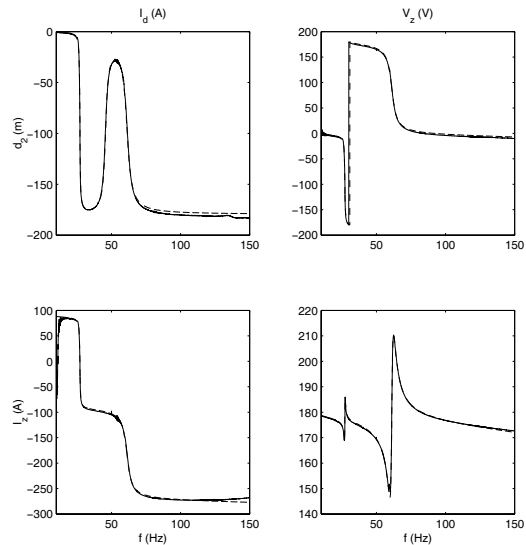

Fig. 10. The simulated (—), and experimental (- -), phase frequency response.

To assess the accuracy of the analytic model, the simulated frequency response is compared to that measured directly from the experimental system. A multivariable frequency response is measured successively from each input to output pair. During the component SISO frequency response measurements, the residual input is set to zero. The magnitude and phase frequency responses are shown respectively in Figures 9 and 10. In the frequency domain, a good correlation can be observed between the analytic model and measured system.

4.3.1. LQR impedance synthesis As discussed in Section 3, a linear quadratic regulator can be designed to command the shunt terminal voltage V_z with a view to minimizing the vibration d_2. An observer is required to estimate the system states from the measured shunt current I_z.

Based on the physical model (including external gains) that was validated in the previous subsection, and referring to the notation introduced in Section 3, an LQR gain matrix was designed to minimize the following performance function,

$$J = \int_{-\infty}^{\infty} \left\{ d_2^2(t) + k_v V_z^2(t) + k_d \left(d_1(t) - d_2(t) \right)^2 \right\} dt, \tag{8}$$

where the factor $k_d = 1$ and $k_v = 1 \times 10^{-7}$. A Kalman observer was designed to estimate the system state $x_g(t)$ utilizing the measured shunt transducer current I_z and control signal V_z. Referring to Section 3.1, the disturbance and output noise process covariance matrices, $\mathbf{Q}_n$ and $\mathbf{R}_n$, were chosen to be 100 and 0.1 respectively. Such a weighting, although not quantitative, expresses a moderate confidence in the fidelity of the measured variable I_z.

By concatenating the LQR gain matrix and Kalman observer, and compensating for the system gains a_3 and a_4, the actual impedance presented to the shunt transducer can be determined. In Figure 12, the complex impedance of the resulting controller is plotted together with that of the negated coil impedance. A negative coil impedance connected to the true coil impedance effectively removes the source impedance from the transducer. The LQG impedance has a tendency to mimic this impedance over a certain frequency range. The pole-zero map of the LQG controller is shown in Figure 11.

After examining the open- and closed-loop pole locations shown in Figure 13, it can be appreciated that the controller is clearly acting to increase the system damping. Corresponding mitigation of the transfer function from an applied disturbance to the measured vibration can be seen in both the frequency domain, Figure 14, and time domain, Figure 15. The action of the additional mass and electromagnetic shunt acts to reduce the single-mass resonant peak by a minimum of 23.2 dB. The shunted electromagnetic transducer reduces the two-mass first and second resonant peaks by 18.7 and 23.6 dB respectively.

The reader may note additional dynamics at 20 and 60 Hz in Figure 14. These dynamics are due to pivot modes of the structure about the base fixture. The stiffening effect of the controller has a tendency to increase the frequency of low-profile pivot and sway modes. Such modes would be absent in a more rigidly supported inertial drive.
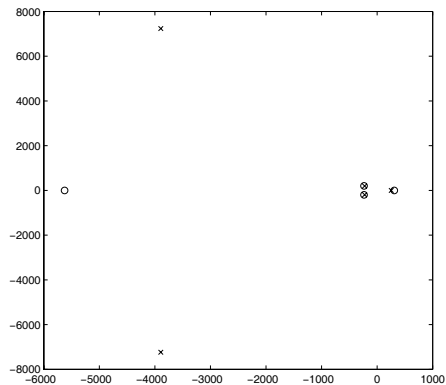

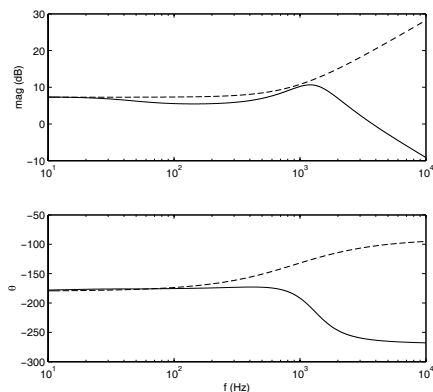Fig. 11. Pole zero map of the LQG impedance.

Fig. 12. Magnitude and phase response of the LQG impedance (—) and negative coil impedance (- -).
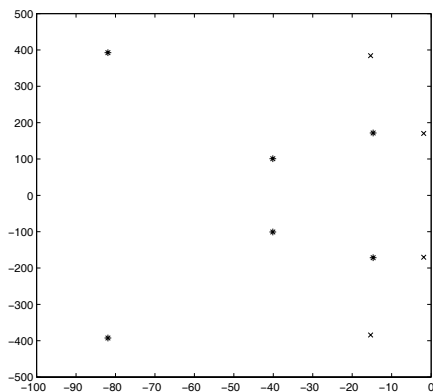

Fig. 13. The open ($\times$) and shunted ($\star$) pole locations. Note that one pair of high-frequency observer poles are not visible within the scope of this plot.

5. CONCLUSIONS

A technique has been presented for the control of vibration using an electromagnetically actuated inertial drive. By viewing the coil current and
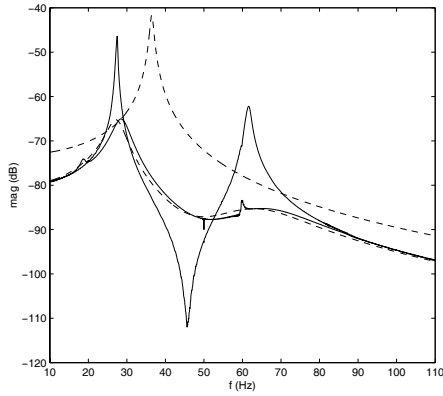
Fig. 14. The single-mass (- -), two-mass (—), experimental shunted (—), and simulated shunted (- -) magnitude frequency response $\frac{d_2(s)}{I_d(s)}$.
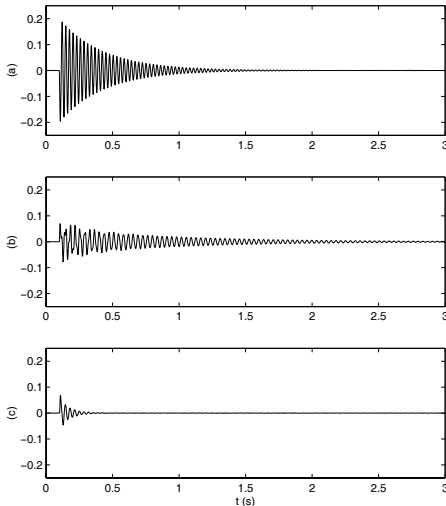

Fig. 15. The single-mass (a), two-mass (b), and shunted two-mass (c) velocity response to a 1 Amp step in I_d.

voltage as system inputs and outputs, standard synthesis techniques were applied to minimize displacement subject to a penalty on the inertial mass travel and applied terminal voltage. Electromagnetic shunt control requires no external sensors, thus significantly reduces the cost, complexity, and sensitivity to transducer failure of active vibration control systems.

Experiments were performed on a simple apparatus representing a scenario where the vibration experienced by a host structure is controlled with a suspended absorber mass and electromagnetic coil. In practice the mass of the absorber is usually limited to about one tenth the host structure. In this regard the experiment is somewhat unrealistic as the mass of the absorber is only slightly less than that of the host mass. The available control authority is directly related to both the size of the mass and the available travel.

After adding the absorber mass, the passive dynamics split the original resonant mode into two lightly damped secondary peaks. By then designing a suitable control impedance, and presenting it to the terminals of the electromagnetic coil, further vibration reduction is achieved by augmenting the passive damping of the secondary modes. As the control design penalizes the absorber mass travel, which increases at low frequencies, the impedance suppresses higher frequency vibration more heavily. The combination of passive and active dynamics reduces the displacement response to a force input by up to 38dB at the frequency of the original resonance.

Future work includes design for multi-mode host structures, coupled multi-drive multi-dimensional systems, and restricted impedance design. The LQG impedance design contains negative reactive components and is unstable in a systems perspective. Although the connection of the coil and control impedance is stable, an inherently stable controller is desirable. It is presently unclear if an unstable controller is necessary to result in effective vibration reduction.

REFERENCES

Brown, R. G. and P.Y.C. Hwang (1997). *Introduction to Random Signals and Applied Kalman Filtering*. John Wiley and Sons Inc.

Inman, D. J. (2000). *Engineering Vibrations*. 2nd ed.. Prentice Hall. ISBN: 013726142X.

Rao, S. S. (1995). *Mechanical Vibrations*. 3rd ed.. Addison-Wesley Publishing Company.

Skogestad, S. and I. Postlethwaite (1996). *Multivariable Feedback Control*. John Wiley and Sons.